RP Materials: Proceedings
Vol. 1, Part 1 (2022) pp. 37–41
e-ISSN:

RESEARCH PLATEAU PUBLISHERS

Cite this article: V.P. Singh, Synthesis of crystalline particles of $LiYO_2$ by sol-gel method and its characterization, *RP Materials: Proceedings* Vol. 1, Part 1 (2022) pp. 37–41.

Original Research Article

Synthesis of crystalline particles of $LiYO_2$ by sol-gel method and its characterization

Vipin Pal Singh
Department of Physics, J.V.M.G.R.R. College, Charkhi Dadri –127306, Haryana India
*Corresponding author, E-mail: vipin78pilania@gmail.com

****Selection and Peer-Review under responsibility of the Scientific Committee of the National Conference on Advanced Engineering Materials (NCAEM 2022).**

ARTICLE HISTORY
Received: 11 Aug. 2022
Revised: 20 April 2023
Accepted: 21 April 2023
Published online: 22 April 2023

KEYWORDS
$LiYO_2$; sol-gel synthesis; nanoparticles.

ABSTRACT
Lithium yttrium oxide ($LiYO_2$) was created using the straightforward sol-gel process with help from citric acid. From a low to a high concentration of lithium precursor, three distinct molar ratios were employed. As opposed to those brought about by solid-state reactions, the purer $LiYO_2$ powders produced by the higher lithium precursor concentration were produced by subduing the unstructured granules generated by the sol-gel process during the heating process. The ideal experimental conditions for the synthesis of sol-gels are a molar ratio of $[Li(CH_3COO)]2H_2O/[Y(NO_3)_36H_2O]$ of 1:3 and 1:2, respectively, at 950°C and 1000°C, with a heating period of 6 hours. LiYO2's reaction and synthesis mechanism was examined and put forth. I discovered that exothermic reactions were created during the process of calcination of dry gel and that the production of $LiYO_2$ was achieved through a straightforward interaction between Li_2O and Y_2O_3.

1. Introduction

The sol-gel approach, which involves preparing ceramic and glass materials in two different states - a solution and a gel - attracts a lot of interest. The sol-gel technology is straightforward and affordable, with a suitable reagent mixture, moderate heating temperature, and numerous opportunities to adjust the characteristics via altering the solution constituents [1, 2]. Thin films, fibres, and granules may be produced using the sol-gel process, and such substances possess a variety of applications in insolating substances, superconducting materials photo catalysis, glasses, dielectric materials, and ferroelectric materials [1–7]. The international community is currently concentrating on the challenges associated with sustainability issues related to lowering the levels of greenhouse gases in the atmosphere. There are a lot of pollutants as a result of the expansion of businesses and technology, notably in the power, transportation, cement-based material, and fossil fuels-based industry. Between 350 and 1000 °C, lithium yttrium oxide ($LiYO_2$), also known as lithium yttriate, is a novel material for the CO_2 absorbent [8]. Compared to Li_2ZrO_3 (450–500°C) [9] and Li_4SiO_4 (up to 720°C) [10], $LiYO_2$ has a greater temperature range. In addition to these, $LiYO_2$ has received extensive study for its potential use in engineering, particularly for its coating for insulation [11], CO_2 absorbing materials [8], Li detectors [12], and electrically conducting materials [11, 13]. Additionally, $LiYO_2$ exhibits exceptional optical and magnetic properties when doped with lanthanides (Eu^{3+}, Tb^{3+}) ions [14-16].

The temperature conditions during synthesis and the type of impurities affect the crystal structure of $LiYO_2$. There are two crystal structures for -$LiYO_2$: a lower symmetric monoclinic structure and a tetragonal structure with $I4_1/amd$ group space [17]. Six oxide ions coordinate the Y ions octahedrally, and Li is essentially surrounded by a plane coordinate polyhedrons [18]. Each YO_6 polyhedron allocates four sides as well as four corners with an adjacent YO_6 polyhedron. Nevertheless, pure $LiYO_2$ has a space group of $P2_1/c$ and is monoclinic at room temperature [14, 19]. The mixed cation layers of closed-packed O_2 are present in the monoclinic structure's somewhat deformed NaCl structure [20]. In the past, $LiYO_2$ was created by solid-state sintering a combination of $LiNO_3$ or Li_2CO_3 with Y_2O_3 precursors at temperatures between 900 and 1400°C with a heating time of 2 to 48 hours [12, 14, 16, 21, 22]. For the synthesis of $LiYO_2$, several preparation techniques, including spark-plasma sintering (SPS), has recently drawn a lot of attention [11]. To my knowledge, $LiYO_2$ has not yet been synthesised via a sol-gel method. This research looked on the sol-gel method of $LiYO_2$ synthesis. This procedure has been carried out to improve the precursor powder's chemical homogeneity and reactivity.

2. Materials and methods

$LiYO_2$ particles were made using the sol-gel technique. The compounds, viz. $Li(CH_3COO).2H_2O$ and $Y(NO_3).36H_2O$ were utilised as starting materials in a conventional synthesis procedure. The starting charges were dissolved in aqueous citric acid monohydrate $C_6H_8O_7.H_2O$ solution stoichiometrically with excess Li precursor. The initial sols were made by dissolving $Li(CH_3COO)$ and $Y(NO_3)_3$ in distilled water in three distinct molar ratios (1:1, 1:2, and 1:3) together with an

equivalent amount of citric acid in a water-based solution (1.2 mol L^{-1}). The mole ratios for both Y as well as Li predecessors in the study were kept at 1:1, 1:2, and 1:3, respectively. Weighing and dissolving the respective masses in water. The water to total precursor mass ratio was set at 2.9. To improve the homogeneity of the mixtures, they were agitated at 27°C for 30 minutes. In order to stabilise the solution, the homogeneous mixture was further agitated for 30 minutes at room temperature after the water-based solution of citric acid is gradually added. After that, the mixture was heated to 80°C in a water bath while being constantly stirred to produce the transparent viscous gel.

To make xerogel, at 90°C for 125 hours, the gel was dried. In order to produce swollen powders, Additionally, for 6 hours, these xerogels were heated to 180°C. The as-prepared xerogels were heated up between 700 to 1200°C at a rate of 5°C/min while being held at various temperatures. Using an X-ray diffractometer, it was established what $LiYO_2$ looked like in terms of phase structure and purity.

The starting material was subjected to DSC/TGA analysis under a 10 mL/min air circulation at a heating rate of 15–30 K/min from 27°C to 1500°C. Sol-gel component combinations were used to create raw powders. XRD pictures were captured, while FT-IR spectra were obtained using the FT-IR spectro-photo-meter. Scanning electron spectroscopy was used to analyse the microstructure.

3. Results and discussion

Figure 1 displays outcomes of TGA and DSC on samples that were made with molar ratios of 1:1, 1:2, and 1:3 and heated for 6 hours at 175°C. The primary exothermic processes, which can be attributed to breakdown of nitrites, acetates, and citrates utilised as detoxifying compounds, take place between 220 and 750 °C [22, 23]. Peaks on DSC curves rise when the molar ratio of the Y prerequisite decreases. It is because an exothermic process is significantly influenced by the citrate-nitrate ions ratio (*c*/*n*) [24].

Citric acid was released at 400°C for both of the initial pair of samples (1:1 and 1:2), which led to the first large peak, and it was caused by the breakdown of citric acid at 385°C for the final sample [22]. According to Singh et al. [24], the exothermic redox reaction produced by annealing xerogel at 180°C for 5 hours causes citric acid to be converted to aconitic acid ($C_6H_6O_6$) and then to itaconic acid ($C_5H_6O_4$), causing the precursor to swell. Within samples having molar ratios of 1:2, 1:3, which correspond to 482 and 535°C, respectively, the second main peak can be attributed to the creation of Li_2O at temperatures over 477°C [26]. The decarburization of the disintegrated products is what causes the event to occur at 600°C (or 627°C for sample 1:1) [22]. For 1:1 and 1:3, these activities continue at around 1000°C, while they were seen sooner in the 1:2 molar ratio sample (850°C). Endothermic peaks for 1:1, 1:2, and 1:3 are shown at 824, 827, and 837°C, respectively.

The absence of the peaks at 1030 and 1339°C for sample with molar ratio 1:3 in the other samples may be understood via responses taking place among too many gases as a result of an increase in the *c*/*n* ratio or an increase in ambient gases. The TGA curve shows no weight loss at the same temperature.

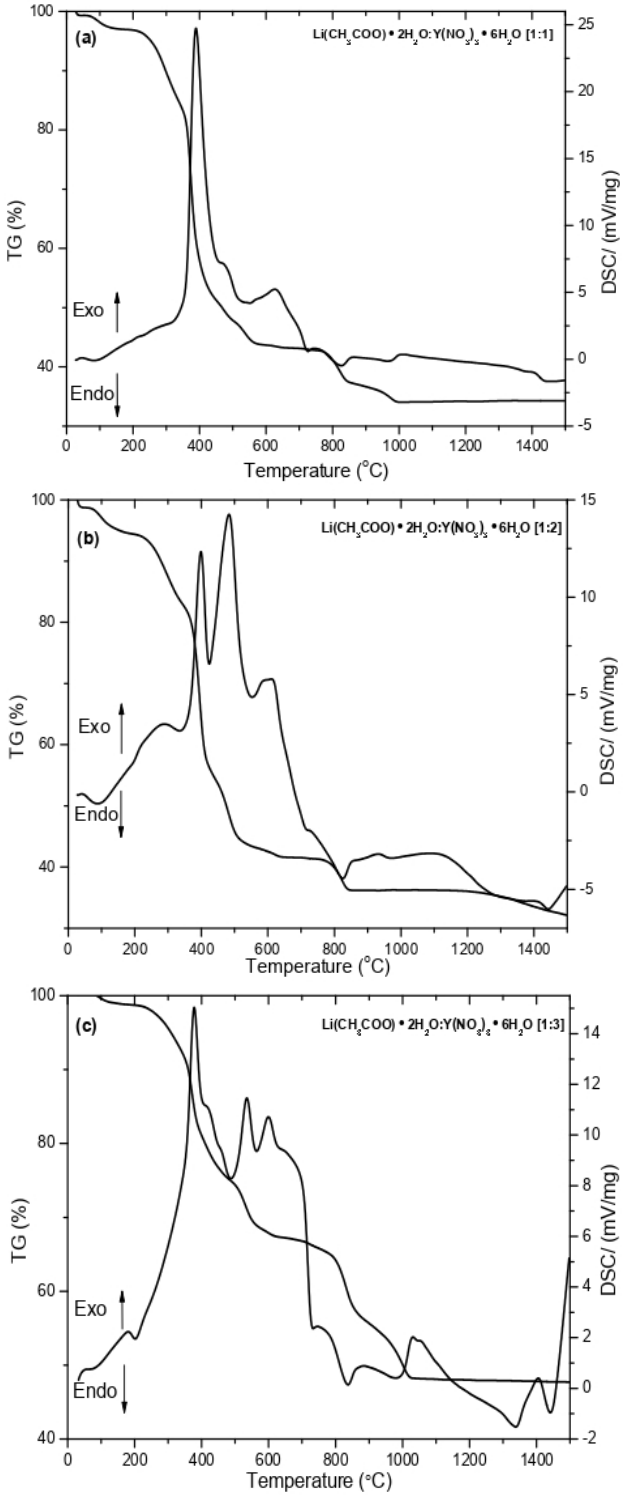

Figure 1: Samples prepared at various mole ratios are shown in (a) 1:1, (b) 1:2, and (c) 1:3 DSC/TGA curves.

Peaks (weak for 1:1 and 1:2) at 1400°C may have occurred by Li being released at a high temperature. Also, as seen in the TGA curves, the weight of the samples decreased by 63.45% for a 1:1 decomposition, 66.65% for a 1:2 decomposition, and 52.54% for a 1:3 decomposition. The breakdown of leftover water, nitrate, and acetate ions, on the other hand, can be the reason why all samples lost weight up to 350°C [23].

FT-IR $LiYO_2$ characterization: FT-IR was used to analyse the ambient temperature spectrum of the 90°C together with-dried gel after 125 hours, the 175°C heated substance, as well as the 1000°C annealing for a 1:2 samples ratio. Figure 2 illustrates the infrared spectrum characteristic of $LiYO_2$, which shows a broad spectrum close to 3450 cm^{-1} that is related via the O-H vibratory stretching mode of water [27]. The O-H vibrations are found in sample annealed to 1000°C because the Li^+ ion is susceptible to wetness [28]. Citric acid's C-H and COO-H stretching motions may be responsible for a shoulder width between 3000 and 2800 cm^{-1}, which suggests no compounds were still present until 125 hours later. A deeper look at the frequency bands at 3075, 2642, and 2540 cm^{-1} as well as the usual oscillation at 1715 cm^{-1} leads to this finding. In addition, the region of 1600 to 825 cm^{-1} was where groups of carboxylic acids and nitrogen compounds showed peak levels [29]. The noteworthy CO_2 vibrational peaks are seen around 1630-1420 cm^{-1} during heating at 175°C for 6 hours. The peak values have reached lowest point around 800°C, thus being consistent with the crystallisation of $LiYO_2$, as shown by DSC graphs. Following the heating process at 1000°C, $LiYO_2$ could potentially be the cause of persistent peak between 1089 and 400 cm^{-1}. In comparison, the as-calcined $LiYO_2$ generated in the present investigation's FT-IR spectrum exhibits an identical trend as the similar structure of aluminium oxide hydroxide or diaspore (-AlOOH), exhibiting three different regions split by significant discrepancies [30]. The Y-O octahedron vibration modes are consistent with the 1st regime at 864-519 cm^{-1}, the Y-OLi bending mode with the second region at 1474-1089 cm^{-1}, and the O-H stretched oscillation with the third regime at or over 3400 cm^{-1}. After annealing from 800°C to 1000°C, the characteristic FT-IR spectrum of $LiYO_2$ can be anticipated. DSC-TG curves also demonstrate $LiYO_2$ crystallisation at temperatures greater than 800°C.

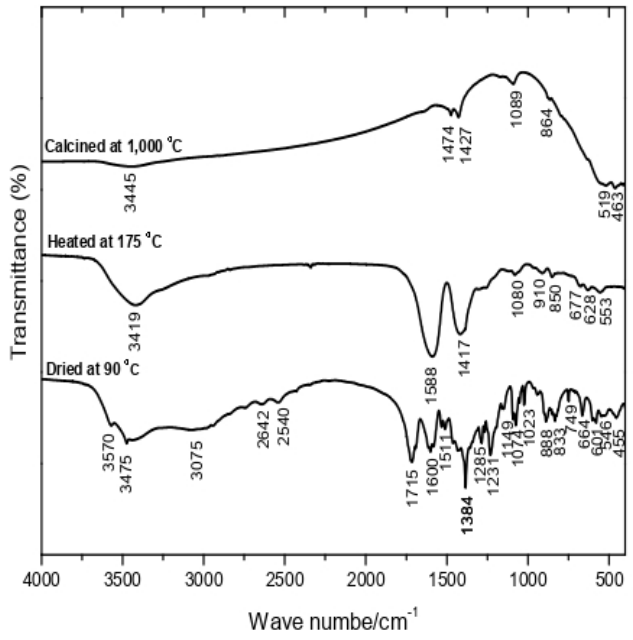

Figure 2: FT-IR spectra of 1:2 mole ratio gels that were heated to 175°C, dried at 90°C, and calcined at 1000°C.

Every sample was heat treated at various temperatures and at constant times, according to XRD analysis. The XRD patterns of samples generated at a 1:1 mole ratio at 700-1200°C with hold periods of two and four hours are shown in Figure 3. $LiYO_2$ powders generated with excessive Li precursor ratios up to 1000°C are shown in Figure 4 as XRD patterns. We may infer from the XRD results that Y_2O_3 begins to crystallise at 700°C, and $LiYO_2$ peaks also begin to form. This conclusion is in good agreement with phase shifts shown in DSC/TGA investigations and the reaction pathways depicted above. The XRD patterns indicate that Y_2O_3 is a predominant crystalline in all mole ratios when the temperature is raised to 700°C. Weak intensity $LiYO_2$ peaks began to form at 800°C, particularly in samples with an abundance of Li precursor. This correlates to the beginning of $LiYO_2$ crystallisation, as determined by the heat treatment investigations. Above this benchmark temperature, the ratio of one to one of released lithium oxide occurs around 1200°C, with no anticipated peak of $LiYO_2$ (See Figure 3). The XRD results for samples with an excessive amount of Li precursor are nearly same, and for materials with 1:2 and 1:3 molar proportions, respectively, complete crystallisation of $LiYO_2$ takes place at 950 to 1000°C.

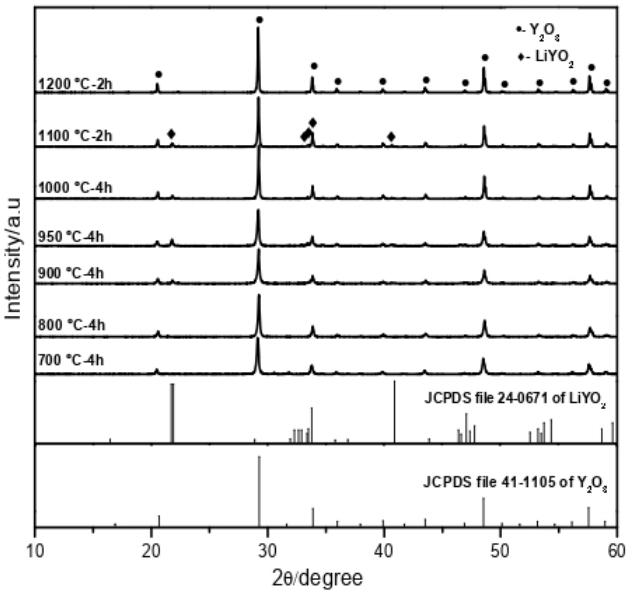

Figure 3: Samples generated at a 1:1 mole ratio as seen in XRD patterns.

In this work, only the patterns with a 1:3 molar ratio are reported (Figure 4). Furthermore, it is clear that $LiYO_2$ must be synthesised at low temperatures, which necessitates a large quantity of Li antecedent and a protracted holding period, which is necessary for the development of particle sizes. As a result, after 6 hours of holding, the pure $LiYO_2$ phase was achieved at 950°C (1:3) and 1000°C (1:2). Compared to high sintering solid-state reaction techniques, the aforementioned temperatures are considerably smaller, which were conducted at 1200°C for 15 hours [12] and 1400°C for 4 hours [21]. If not, $LiYO_2$ has to be synthesised at 900°C over the course of substantially longer annealing times (12–48 hours) [16].

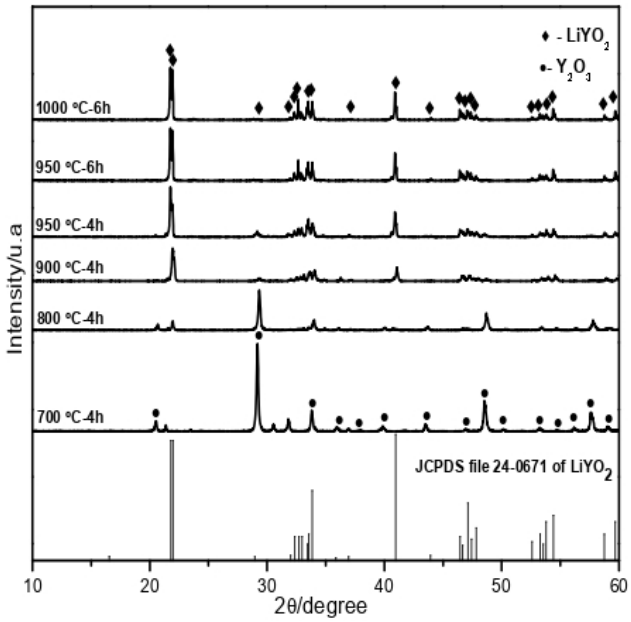

Figure 4: X-ray diffractograms of samples generated at a mole ratio of 1:1 and calcined at various temperatures and holding times.

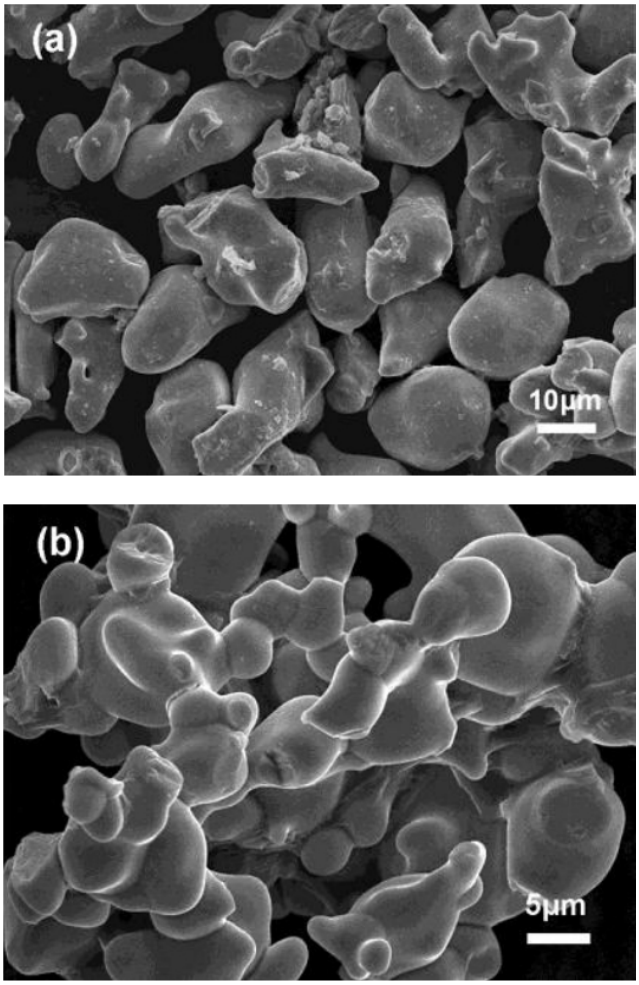

Figure 5: A SEM image of $LiYO_2$ that was calcined at 950°C for 6 hours (1:3) and at 1000°C for 6 hours (1:2).

The SEM illustrations of the $LiYO_2$ granules as-prepared at 950°C (1:3) and 1000°C (1:2) in Figure 5 demonstrate that the average size of the particles of the synthesised granules is below 25 m with a homogenous size variation. This amazing grain development may be caused by the relatively lengthy holding time and modest calcination rate (5°C/min). A substantial aggregation of particles at 1000°C in a sample ratio of 1:2 is seen in addition to the varied forms in Figure 5 [22, 23]. These clumped particles require more research to be done on them. No Y_2O_3 contamination on the surface of $LiYO_2$ grains is seen in comparison to earlier research [12].

4. Conclusions

Without complexing the metal precursors, monoclinic $LiYO_2$ crystals were created utilising a straightforward sol-gel method and citric acid. For samples having an excessive amount of Li precursor, at 1:3 and 1:2 molar ratios, the ideal synthesis temperature is 950 to 1000°C with a holding period of 6 hours. Itaconic acid, which is produced from citric acid, served as the fuel for the redox combustion technique between citrate and nitrate. Lithium oxide and yttria simply reacted to produce $LiYO_2$. Compared to the conventional solid-state reaction approach, the synthesis temperature is substantially shorter and the duration of holding time is comparatively less. Without any yttria contamination, the heat treatment causes an increase in particle size. Furthermore, FT-IR research shows that no compounds between acid and metal oxides were generated during the sol-gel process. Also, it is demonstrated that many vibration modes within the structure are deepened, which requires further research.

References

[1] M. Crişan, A. Braileanu, M. Răileanu, M. Zaharescu, D. Crişan, N. Dragan, M. Anastasescu, A. Ianculescu, I. Niţoi, V.E. Marinescu, S.M. Hodorogea, Sol–gel S-doped TiO_2 materials for environmental protection, *J. Non-Cryst. Solids* **354** (2008) 705–711.

[2] Z. Xiu, M. Lu, S. Liu, G. Zhou, B. Su, H. Zhang, Barium hydroxyapatite nanoparticles synthesized by citric acid sol-gel combustion method, *Mater. Res. Bullet.* **40** (2005) 1617-1622.

[3] B.D. Mac Craith, C. Mc Donagh, A.K. Mcevoy, T. Butler, G. O'Keeffe, V. Murphy, Optical chemical sensors based on sol-gel materials: Recent advances and critical issues, *J. Sol-Gel Sci. Technol.* **8** (1997) 1053–1061.

[4] S.H. Xie, J.Y. Li, R. Proksch, Y. M. Liu, Y.C. Zhou, Y.Y. Liu, Y. Ou, L.N. Lan, Y. Qiao, Nanocrystalline multiferroic $BiFeO_3$ ultrafine fibers by sol-gel based electrospinning, *Appl. Phys. Lett*. **93** (2008) 222904.

[5] O. Cakiroglu, L. Arda, Y.S. Hascicek, High voltage breakdown studies of sol–gel MgO–ZrO_2 insulation coatings under various pressures at 298 K and 77 K, *Physica C* **422** (2005) 117–126.

[6] C.D.E. Lakeman, D.A. Payne, Sol-gel processing of electrical and magnetic ceramics, *Mater. Chem. Phys*. **38** (1994) 305–324.

[7] J. Zhang, L. Gao, Synthesis of antimony-doped tin oxide (ATO) nanoparticles by the nitrate-citrate combustion method, *Mater. Res. Bullet*. **39** (2004) 2249–2255.

[8] M. Yamauchi, Y. Itagaki, H. Aono, Y. Sadaoka, Lithium carbonate-metal oxide mixtures and its application for a CO_2 absorbent, *J. Ceram. Soc. Japan* **114** (2006) 648–650.

[9] K. Nakagawa, T. Ohashi, A novel method of CO_2 capture

from high temperature gases, *J. Electrochem. Soc*. **145** (1998) 1344–1346.
[10] M. Kato, K. Nakagawa, New series of lithium containing complex oxides, lithium silicates, for application as a high temperature CO_2 absorbent, *J. Ceram. Soc. Japan* **109** (2001) 911–914.
[11] M. Nagura, A. Suzuki, K. Sasaki, T. Terai, Chemical stability of $LiYO_2$ as an insulating material, *Fusion Eng. Design* **85** (2010) 1098–1101.
[12] J. Wu, L. Yamarte, A. Petric, Fabrication of a lithium sensor based on $LiYO_2$ by liquid phase processing, *J. Electroceramics* **9** (2002) 57-66.
[13] Y. Zou, A. Petric, Structure and conductivity of zirconium-doped polycrystalline lithium yttrium oxide, *Mater. Res. Bullet*. **28** (1993) 1169-1175.
[14] M.D. Faucher, Ph. Sciau, J-M. Kiat, M-G Alves, F. Bouree, Refinement of the monoclinic and tetragonal structures of Eu^{3+}-doped $LiYO_2$ by neutron diffraction at 77 and 383 K Differential Scanning Calorimetry, and Crystal Field Analysis, *J. Solid State Chem*. **137** (1998) 242–248.
[15] M.D. Faucher, O.K. Moune, M-G Alves, B. Piriou, Ph. Sciau, M. Pham-Thi, Optical and crystallographic study of Eu^{3+} and Tb^{3+} doped $LiYO_2$: Phase transition, luminescence efficiency and crystal field calculation, *J. Solid State Chem*. **121** (1996) 457–466.
[16] Y. Hashimoto, M. Wakeshima, K. Matsuhira, Y. Hinatsu, and Y. Ishii, Structures and magnetic properties of ternary lithium oxides $LiRO_2$ (R = Rare Earths), *Chem. Mater*. **14** (2002) 3245–3251.
[17] H. Glaum, S. Voigt, R.Z. Hoppe, Two representatives of the α-$LiFeO_2$ type: $LiInO_2$ and α-$LiYbO_2$, *Anorg. Allg. Chem*. **598** (1991) 129.
[18] Y.B. Kuo, W. Scheld, R. Hoppe, To the knowledge of thealpha-$LiFeO_2$ type: An examination of $LiScO_2$ and $NaNdO_2$, *Zeitschrift für Kristallographie* **164** (1983) 121-127.
[19] M.J. Weber, *Handbook of Optical Materials*, CRC Press, Boca Raton (2003) pp. 1-512.
[20] X. Zhang, D.A. Jefferson, R.M. Lambert, Structure and performance of $LiYO_2$ methane coupling catalysts: Active phases and decay mechanisms, *J. Catalysis* **141** (1993) 583–594.
[21] S. Chockalingam, D.A. Earl, Microwave sintering of Si_3N_4 with $LiYO_2$ and ZrO_2 as sintering additives, *Mater. Design* **31** (2010) 1559–1562.
[22] K. Devi, R. Choudhary, A.K. Satsangi, R.K. Gupta, Sol-gel synthesis and characterisation of nanocrystalline yttrium aluminum garnet nanopowder, *Def. Sci. J*. **58** (2008) 545–549.
[23] K. Suryakala, G.P. Kalaignan, T. Vasudevan, Synthesis and electrochemical improvement of nanocrystalline $LiMn_{2-x}MgXO_4$ powder using sol-gel method, *Int. J. Electrochem. Sci*. **1** (2006) 372–378.
[24] K.A. Singh, L.C. Pathak, S.K. Roy, Effect of citric acid on the synthesis of nano-crystalline yttria stabilized zirconia powders by nitrate-citrate process, *Ceram. Int*. **33** (2007) 1463-1468.
[25] S.R. Jain, K.C. Adiga, V.R. Pai Verneker, A new approach to thermochemical calculations of condensed fuel-oxidizer mixtures, *Combust Flame* **40** (1981) 71–79.
[26] Y.H. Hu, E. Ruckenstein, Nanostructured Li_2O from LiOH by electron-irradiation, *Chem. Phys. Lett*. **430** (2006) 80-83.
[27] A.L. Costa, L. Esposito, V. Medri, A. Bellosi, Synthesis of Nd-YAG material by citrate-nitrate sol-gel combustion route, *Adv. Eng. Mater*. **9** (2007) 307-312.
[28] R.K. Kotnala, J. Shah, B. Singh, S. Singh, S.K. Dhawan, A. Sengupta, Humidity response of Li-substituted magnesium ferrite, *Sensors and Actuators B: Chem*. **129** (2008) 909–914.
[29] M. Blosi, S. Albonetti, M. Dondi, A.L. Costa, M. Ardit, G. Cruciani, Sol-gel combustion synthesis of chromium doped yttrium aluminum perovskites, *J. Sol-Gel Sci. Technol*. **50** (2009) 449-455.
[30] R. Demichelis, Y. Noel, B. Civalleri, C. Roetti, M. Ferrero, R. Dovesi, The vibrational spectrum of α-AlOOH diaspore: an ab initio study with the crystal code, *J. Phys. Chem. B* **111** (2007) 9337–9346.